dorsal horn during postnatal development. Neuroscience 99 : 549−556, 2000.
5) Jiang N, Furue H, Katafuchi T et al : Somatostatin directly inhibits substantia gelatinosa neurons in adult rat spinal dorsal horn in vitro. Neurosci Res 47 : 97−107, 2003.
6) Kim SJ, Chung WH, Rhim H et al : Postsynaptic action mechanism of somatostatin on the membrane excitability in spinal substantia gelatinosa neurons of juvenile rats. Neuroscience 114:1139−1148, 2002.
7) Marker CL, Stoffel M, Wickman K : Spinal G-protein-gated K^+ channels formed by GIRK1 and GIRK2 subunits modulate thermal nociception and contribute to morphine analgesia. J Neurosci 24 : 2806−2812, 2004.
8) Mollenholt P, Rawal N, Gordh TJr et al : Intrathecal and epidural somatostatin for patients with cancer. Analgesic effects and postmortem neuropathologic investigations of spinal cord and nerve roots. Anesthesiology 81 : 534−542, 1994.
9) Murase K, Nedeljkov V, Randi M:The actions of neuropeptides on dorsal horn neurons in the rat spinal cord slice preparation : an intracellular study. Brain Res 234 : 170−176, 1982.
10) Chung K, Briner RP, Carlton SM et al : Immunohistochemical localization of seven different peptides in the human spinal cord. J Comp Neurol 280 : 158−170, 1989.
11) Mizukawa K, Otsuka N, McGeer PL et al : The ultrastructure of somatostatin-immunoreactive cell bodies, nerve fibers and terminals in the dorsal horn of rat spinal cord. Arch Histol Cytol 51 : 443−452, 1988.
12) Krisch B : Somatostatin-immunoreactive fiber projections into the brain stem and the spinal cord of the rat. Cell Tissue Res 217 : 531−552, 1981.
13) Tessler A, Himes BT, Gruber-Bollinger J, Reichlin S : Characterization of forms of immunoreactive somatostatin in sensory neuron and normal and deafferented spinal cord. Brain Res 370 : 232−240, 1986.

Neuroscience Letters 494 (2011) 161–164

Contents lists available at ScienceDirect

Neuroscience Letters

journal homepage: www.elsevier.com/locate/neulet

Electrophysiological analysis of vulnerability to experimental ischemia in neonatal rat spinal ventral horn neurons

Hiroyuki Honda, Hiroshi Baba, Tatsuro Kohno*

Division of Anesthesiology, Niigata University Graduate School of Medical and Dental Sciences, 1-757 Asahimachi, Chuo-ku 951-8510, Niigata, Japan

ARTICLE INFO

Article history:
Received 14 December 2010
Received in revised form 1 March 2011
Accepted 2 March 2011

Keywords:
Patch clamp
Spinal cord ischemia
Spinal motoneuron

ABSTRACT

To clarify the vulnerability of spinal motoneurons to excitotoxicity, we analyzed the agonal current induced by experimental ischemia in ventral lamina IX neurons of spinal cord slices from neonatal rats by using whole-cell patch-clamp. Ischemia was simulated *in vitro* by oxygen/glucose deprivation. Superfusion with ischemia-simulating medium elicited an agonal inward current, which was initially slow and then became rapid. We compared 8-, 9-, 10-, 11-, and 12-day postnatal rats and found age-dependent shortening of the latency of the rapid inward current. Furthermore, the membrane capacitance (Cm) and resting membrane potential (RMP) of the lamina IX neurons demonstrated significant negative correlations with the latency of the rapid inward current. Logistic regression analysis showed that postnatal age, Cm, and RMP were independent contributing factors to ischemic vulnerability. These results suggest that not only cell volume and ionic balance but also early postnatal maturation of the intracellular environment is vital for developing vulnerability to excitotoxicity.

Excitotoxicity is an important mechanism of neuronal death, implicated in the pathogenesis of ischemia, trauma, and neurodegenerative disorders [8,10,15]. Excitotoxic injury is mediated by glutamate, a major excitatory neurotransmitter. During pathologic insult, glutamate excessively accumulates in the extracellular space and stimulates the neurons through ionotropic receptors [9,11,14,20]; such stimulation leads to neuronal depolarization and irreversible loss of function [17].

Specific regions of the central nervous system are susceptible to developing neuronal damage after excitotoxic injury. In addition, such vulnerability critically depends on postnatal maturation [16]. Spinal cord motoneurons are also known to be particularly vulnerable during ischemia [17]; some of their molecular features are known to play important roles in cell death in degenerative motoneuron diseases [22]. However, factors contributing to the vulnerability of spinal motoneurons to ischemia and changes in susceptibility during maturation have not been well documented.

In vitro ischemia is mimicked by oxygen/glucose deprivation; this preparation has been well established in electrophysiological studies with spinal cord and brain slices [17,18,23–25]. In the present study, we investigated the influence of experimental ischemia on ventral lamina IX neurons in spinal cord slices by using the whole-cell patch-clamp method to clarify parameters contributing to the vulnerability of developing spinal motoneurons.

All experimental procedures involving the use of animals were approved by the Animal Care and Use Committee of Niigata University Graduate School of Medical and Dental Sciences (Niigata, Japan).

Slices of rat spinal cord were prepared as previously described [17]. In brief, neonatal Wistar rats (8–12 days postnatal) were anesthetized with urethane (1.2–1.5 g/kg, intraperitoneal). Dorsal laminectomy was performed, and the lumbosacral segment of the spinal cord was removed. The rats were immediately killed by exsanguination. The spinal cord was placed in pre-oxygenated ice-cold artificial cerebrospinal fluid (ACSF). After cutting all the ventral and dorsal roots near the root entry zone, the pia-arachnoid membranes were removed. The spinal cord was mounted on a metal stage of a microslicer (DTK-1500; Dosaka, Kyoto, Japan) and cut into 500-μm-thick transverse slices. Each spinal cord slice was transferred to a recording chamber and placed on the stage of an upright microscope equipped with an infrared-differential interference contrast (IR-DIC) system (E600FN; Nikon, Tokyo, Japan). The slice was fixed by an anchor and superfused at 4–6 ml/min with ACSF solution equilibrated with a gas mixture of 95% O_2 and 5% CO_2 and maintained at 36 °C by using a temperature controller (TC-324B; Warner Instruments, Hamden, CT, USA). The ACSF solution comprised (in mM): 117 NaCl, 3.6 KCl, 2.5 $CaCl_2$, 1.2 $MgCl_2$, 1.2 NaH_2PO_4, 25 $NaHCO_3$, and 11.5 D-glucose (pH 7.4).

Lamina regions were identified under low magnification (5× objective lens) and individual neurons were identified using a 40× objective lens with an IR-DIC microscope and monitored by a CCD camera (C2400-79H; Hamamatsu Photonics, Hamamatsu, Japan)

* Corresponding author. Tel.: +81 25 227 2328; fax: +81 25 227 0790.
E-mail addresses: kohno-t@umin.net, kohno@med.niigata-u.ac.jp (T. Kohno).

0304-3940/$ – see front matter © 2011 Elsevier Ireland Ltd. All rights reserved.
doi:10.1016/j.neulet.2011.03.003

on a video monitor screen. The size of each recorded neuron was calculated from the arithmetic mean length of the diameter of the long and short axes of the soma intersecting at right angles. Whole-cell voltage-clamp or current-clamp recordings were made from large lamina IX neurons (size, 15–25 μm), which were generally observed in the ventral lateral or ventral medial areas. Whole-cell patch pipettes were constructed from borosilicate glass capillaries (1.5-mm OD; World Precision Instruments, Sarasota, FL, USA). The resistance of a typical patch pipette was 5–10 MΩ when filled with an internal solution composed of (in mM) 135 potassium gluconate, 5 KCl, 0.5 $CaCl_2$, 2 $MgCl_2$, 5 EGTA, 5 HEPES, and 5 ATP-Mg (pH 7.2). After the whole-cell configuration was established, voltage-clamped neurons were held at −70 mV and current-clamped neurons were held at 0 pA. Signals were amplified with an Axopatch 200B amplifier (Molecular Devices, Union City, CA, USA), filtered at 2 kHz, and digitized at 5 kHz. Data were stored and analyzed using a pCLAMP 9.1 data acquisition program (Molecular Devices). Membrane capacitance (Cm) and input resistance (Rin) were measured by applying hyperpolarizing voltage pulses (10 mV) from a holding potential of −70 mV with a duration of 20 ms. Cm was measured by integrating the transient capacitative currents evoked during the voltage-clamp steps. These measurements were used to estimate membrane surface area [21]. We considered the potential at which the holding current becomes zero to be the resting membrane potential (RMP). Neurons with RMPs above −50 mV were removed from the analysis [1,3].

Ischemia was simulated by superfusing the slices with ischemia-stimulating medium (ISM) consisting of ACSF solution, equilibrated with a gas mixture of 95% N_2 and 5% CO_2, in which glucose was replaced with an equimolar concentration of sucrose. Drugs and ISM were applied by perfusion via a three-way stopcock, without changing the perfusion rate or temperature. The solution in the connection tube and recording chamber having a volume of 2.5 ml was completely replaced within 35 s of the initiation of ISM perfusion. After applying the ischemia-simulating medium, we discarded the slice.

Numerical data are represented as mean ± SEM. One-way analysis of variance (ANOVA) with post hoc Tukey's honestly significant difference (HSD) test was used to compare the groups classified according to age. Pearson's correlation coefficients (r) were calculated between latency of rapid inward currents induced by ISM and age or electrophysiological membrane properties. Multiple regression analyses were performed to determine the relative contribution of different variables, and F-test was used to evaluate the significance of all independent variables. Statistical significance was defined as $P < 0.05$. When referring to electrophysiological data, n indicates the number of neurons studied.

Whole-cell voltage-clamp recordings were made from 69 neurons of which 60 exhibited RMPs below −50 mV and were included in analysis. Neuron bodies were round or multipolar, with an average soma size of 20.5 ± 0.3 μm; average Cm, 90.8 ± 4.4 pF; average RMP, −58.1 ± 0.3 mV, and average Rin, 152.4 ± 9.2 MΩ ($n = 60$). Soma size demonstrated a significant positive correlation with Cm ($r = 0.57$, $P < 0.01$).

The lamina IX neurons remained viable up to 12 h in slices perfused with pre-oxygenated ACSF solution. However, all recordings in this experiment were obtained within the first 4 h. When the membrane potential was held at −70 mV, superfusion with ISM produced an outward current of 34.1 ± 6.6 pA in 20% of the 60 neurons examined ($n = 12$); this was followed by an agonal inward current (Fig. 1A). The remaining neurons ($n = 48$) exhibited only the inward current. Meanwhile, in the current-clamp mode, ISM produced agonal depolarization followed by persistent depolarization ($n = 5$, Fig. 1B). When ISM superfusion was continued after the appearance of the agonal depolarization, synaptic activity disappeared, and it could not be returned to its previous state despite

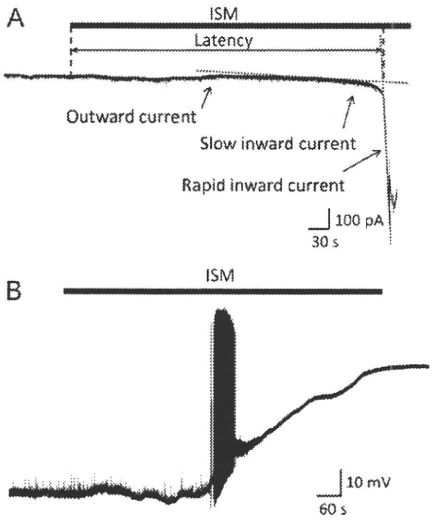

Fig. 1. Agonal current induced by ischemia-simulating medium (ISM) in a representative lamina IX neuron. (A) In the voltage-clamp mode, perfusion with ISM produced an outward current and, subsequently, an agonal inward current at −70 mV in 20% of the neurons examined ($n = 12$). The agonal inward current consisted of a slow and subsequent rapid inward current. The latency of the rapid inward current was measured from the beginning of ISM perfusion to the onset of the rapid inward current, which was estimated by extrapolating the slope of the rapid inward current to the slope of the slow inward current. The current trace shown was obtained from a neuron of an 8-day postnatal rat. (B) In the current-clamp mode, perfusion with ISM produced an agonal depolarization. The resting membrane potential was −61 mV. After the generation of rapid depolarization, the membrane continued to depolarize to 0 mV and synaptic activity disappeared. This trace was obtained from a neuron of a 9-day postnatal rat.

ACSF reperfusion, indicating that ISM resulted in irreversible membrane dysfunction (Fig. 1B). The agonal inward current consisted of a slow followed by a rapid inward current [23]. The onset of the rapid inward current was estimated by extrapolating the slope of the rapid inward current into the slope of the slow current. The latency of the rapid inward current was measured from the onset of superfusion with the ISM to that of the rapid inward current (Fig. 1A). Such a brief superfusion with ISM is known to affect synaptic transmission for several hours in rat hippocampal CA1 neurons; therefore, only the data obtained by its primary application were included in the present study.

Twelve lamina IX neurons in each age group were exposed to ISM. To estimate the influence of an initial outward current, we compared the average age, size, Cm, RMP, Rin, and latency of the rapid inward current. No significant differences were observed in these results between neurons with (10.2 ± 0.5 days, 21.2 ± 0.6 μm, 102.1 ± 7.7 pF, −56.1 ± 1.5 mV, 134.9 ± 12.2 MΩ, 440 ± 23 s, $n = 12$) and without (10.0 ± 0.2 days, 20.3 ± 0.3 μm, 87.9 ± 5.1 pF, −58.6 ± 1.0 mV, 156.8 ± 11.1 MΩ, 454 ± 33 s, $n = 48$) ISM-induced outward currents ($P = 0.65$, 0.24, 0.20, 0.23, 0.35, 0.80, respectively). The differences in soma size and electrophysiological membrane properties between the groups are listed in Table 1. Average latencies of the rapid inward current in the lamina IX neurons were 478 ± 19 s, 448 ± 26 s, 424 ± 32 s, 391 ± 28 s, and 377 ± 18 s on postnatal days 8, 9, 10, 11, and 12, respectively. An obvious age-dependent shortening of the latency of the rapid inward currents was observed (one-way ANOVA, $P < 0.05$; post hoc Tukey's HSD test, P8 versus P12, $P < 0.05$) (Fig. 2). Because age was not found to be a significant factor in the correlation between membrane properties and latency of the rapid inward current, we analyzed these results without grouping by age. Cm of the lamina IX neurons demonstrated a significant negative correlation with the latency of the rapid inward current ($r = -0.41$, $P < 0.01$) (Fig. 3A). Furthermore, RMP of the neurons also exhibited a sig-

Table 1
Comparison of the soma size and electrophysiological membrane properties classified according to postnatal age.

Postnatal days	P 8	P 9	P 10	P 11	P 12	*P* value
n	12	12	12	12	12	
Size (μm)	20.3 ± 0.6	20.4 ± 0.7	21.5 ± 0.9	19.7 ± 0.4	20.5 ± 0.6	0.45
Cm (pF)	83.0 ± 6.8	80.2 ± 7.7	107.2 ± 15.4	87.2 ± 7.2	96.3 ± 9.4	0.30
RMP (mV)	−60.8 ± 2.1	−57.8 ± 1.7	−57.2 ± 2.1	−56.5 ± 1.5	−58.2 ± 1.9	0.56
Rin (MΩ)	146.8 ± 19.9	139.5 ± 18.6	150.8 ± 27.0	183.9 ± 17.4	141.0 ± 19.6	0.55

There was no significant difference in soma size and membrane properties by one-way ANOVA among the postnatal age groups. Cm: membrane capacitance; RMP: resting membrane potential; Rin: input resistance. Data are shown as mean ± SEM. *n* refers to the number of neurons studied.

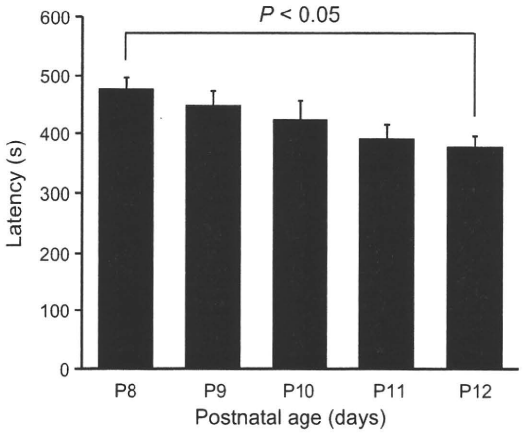

Fig. 2. Comparison of the latency of the rapid inward current induced by experimental ischemia between the different age groups. An obvious age-dependent shortening of the latency of the rapid inward current was observed (one-way analysis of variance $P < 0.05$; post hoc Tukey's honestly significant difference test, P8 versus P12, $P < 0.05$).

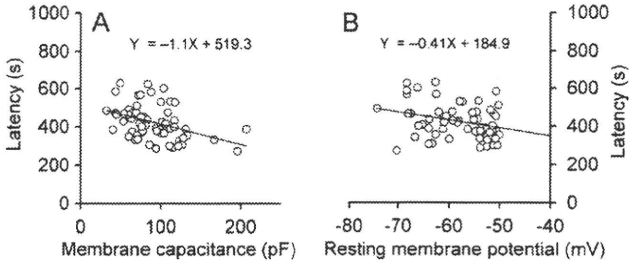

Fig. 3. Correlation between electrophysiological membrane properties and the latency of the rapid inward current as generated by ISM perfusion in lamina IX neurons (8–12 days postnatal, $n = 60$). Membrane properties were measured prior to ISM perfusion. (A) There was a negative correlation between membrane capacitance and latency ($r = -0.41$, $P < 0.01$). (B) There was also a negative correlation between resting membrane potential and latency ($r = -0.30$, $P < 0.05$).

nificant negative correlation with the latency of the rapid inward current ($r = -0.30$, $P < 0.05$) (Fig. 3B). On the other hand, Rin did not correlate with the latency ($r = -0.11$, $P > 0.05$). Logistic regression analysis showed that postnatal age, Cm, and RMP were independent contributing factors to vulnerability to ISM exposure (Table 2). The adjusted determination coefficient was 0.42, and the *F*-test showed the fitted line to be significant ($P < 0.00001$).

In this study, we reported three novel findings. First, we have demonstrated age-dependent shortening of the latency of the rapid inward current in the spinal lamina IX neurons. Surprisingly, this vulnerability develops quickly over a short neonatal period. Second, we found that RMP and Cm correlate with the latency of the rapid inward current. Third, we confirmed that age, Cm, and RMP are independent factors contributing to vulnerability.

It is generally accepted that ISM superfusion produces an outward current followed by an agonal inward current, which comprises a slow and subsequently rapid inward current. Once ISM is applied, intracellular ATP concentration decreases and intracellular Ca^{2+} concentration increases, which elicits an outward current in a portion of neurons because of the activation of both ATP-sensitive K^+ channels and Ca^{2+}-dependent K^+ channels [25]. Glutamate accumulates in the interstitial space and partially mediates the slow inward current via receptor activation [23]. In addition, the increase in intracellular Ca^{2+} and extracellular K^+ concentrations due to the inhibition of Na^+/K^+-ATPase activity contributes to the production of slow current [23]. Meanwhile, the rapid inward current is accompanied by a sudden increase in the intracellular Ca^{2+} concentration [23]. In addition to the action of glutamate receptors, the increase in the intracellular Ca^{2+} concentration is associated with Ca^{2+} influx via voltage-dependent Ca^{2+} channels, reversed operation of Na^+/Ca^{2+} transporters, and Ca^{2+} release from intracellular storage sites [7]. Furthermore, the rapid inward current is likely to be due to a nonselective increase in neuronal permeability of all participating ions; this will occur only in pathological conditions such as ischemia [23].

In this study, we found that the latency of ISM-induced rapid inward current drastically shortened between postnatal days 8 and 12. A parallel age dependency has also been reported in the spinal lamina V dorsal horn neurons of rats [6]. These findings suggest that maturation-dependent spinal neuronal vulnerability to ischemia is determined in the early postnatal period. Because no significant differences were found in soma size or passive electrophysiological membrane properties among the age groups, we conclude that age-dependent shortening of the latency is not because of the effects of increase in cell size or alteration in membrane properties. Interestingly, the number of ionotropic glutamate receptors is known to initially increase during the first 7 postnatal days prior to a decline to adult levels [4], which raises the possibility that glutamate, which plays a major role in excitotoxic cell death, is not

Table 2
Relationships between latencies of rapid inward current and contributing factors evaluated by multiple regression analysis.

	Regression coefficient	95% CI for regression coefficient		
		Lower	Upper	*P* value
Age (days)	−0.345	−0.574	−0.115	0.004
Cm (pF)	−0.015	−0.024	−0.006	0.038
RMP (mV)	−0.054	−0.104	−0.003	0.002

The adjusted determination coefficient was 0.42 and the *F*-test showed the fitted curve to significant ($P < 0.00001$). Postnatal age, Cm and RMP were independent contributing factors of vulnerability to ISM exposure.

involved in the development of vulnerability to ischemia during maturation.

Spinal motoneurons have large somas and long axonal processes; these characteristics greatly differ from those of many other types of neurons. Since these large neurons have high-energy demands for maintaining cytoskeletal components, they may be more susceptible to ischemic insult. Here, we demonstrated a significant correlation between Cm and the latency of ISM-induced rapid inward currents. Cm, which represents the surface areas of the recorded neurons, correlated with soma size, suggested the possibility that latency might also correlate neuronal volume; indeed, vulnerability to experimental ischemia with cell volume has been reported in the spinal cord ventral horn neurons [17,19] and the brain [13]. However, no significant correlation has been observed between the Cm and latency of rapid inward currents in the spinal dorsal horn neurons [17] while in the brain, large CA3 pyramidal neurons display high tolerance to ischemia [12]. These inconsistent findings implicate the involvement of other factors contributing to neuronal vulnerability.

In addition, we found a weak but significant correlation between RMP and current latency. In general, deprivation of oxygen and glucose impairs mitochondrial ATP production, thus compromising ionic gradients across the neuronal cell membrane [9]. In response to ISM superfusion, the membrane is gradually depolarized, leading to the activation of voltage-dependent calcium channels. Ca^{2+} accumulates in the intracellular space, subsequently inducing neuronal death [5,9]. Our finding suggests that lamina IX neurons with a higher hyperpolarized RMP, distant from the threshold of voltage-dependent Ca^{2+} channels, are more resistant to ischemic insults. However, the fact that all recordings were obtained at −70 mV raises doubts about RMP-dependent shortening of latency. One explanation is that incompletely voltage-clamped membrane distant from the patch electrode contributes to RMP-dependent vulnerability.

Furthermore, with logistic regression analysis, the contribution of postnatal age to susceptibility to experimental ischemia was found to be independent of the electrophysiological membrane properties. The determination coefficient (the squared value of the multiple correlation coefficient) has a value of 0.42, indicating that almost half of the variation in neuronal vulnerability for ischemia is explained by these factors. It has been reported that the number of mitochondria increases 4-fold between postnatal days 1 and 21, and is paralleled by an increase in respiratory enzyme content per mitochondrion [2]. This raises the possibility that postnatal development-dependent changes in the intracellular environment, such as metabolism or mitochondrial function, are involved in neuronal vulnerability.

Our study had certain limitations. First, we did not evaluate the age-dependent effect in adult rats. In order to identify large lamina IX neurons under IR-DIC microscope, it was necessary to exclude older rats, whose spinal neurons are obscured by highly developed fibrous tissue. Second, there was a possibility that the presence of the ISM-induced outward current affected the estimation of the slope of the slow inward current and thus the latency of the raid inward current. However, because the slope of the rapid inward current was quite precipitous, we considered that an error in determining the slope of the slow inward current would not greatly affect the estimation of the onset of the rapid inward current. Third, because the spinal lamina IX neurons studied included propriospinal interneurons, our observations may not exclusively apply to spinal motoneurons. Further studies with adult rat spinal motoneurons are required.

In conclusion, we determined that age, cell volume, and RMP may independently contribute to the susceptibility of spinal ventral lamina IX neurons to ischemia. These results emphasize that each contributing factor must be taken into consideration while evaluating spinal motoneuronal injury during development. We further propose that early postnatal maturation of the intracellular environment is an important factor affecting the development of vulnerability to excitotoxicity.

Acknowledgements

This work was supported by Grants-In-Aid for Scientific Research (grant numbers 20390414 and 21791438) from the Ministry of Education, Culture, Sports, Science and Technology of Japan, Tokyo, Japan.

References

[1] T. Aoyama, S. Koga, T. Nakatsuka, T. Fujita, M. Goto, E. Kumamoto, Excitation of rat spinal ventral horn neurons by purinergic P2X and P2Y receptor activation, Brain Res. 1340 (2010) 10–17.
[2] K. Blomgren, H. Hagberg, Free radicals, mitochondria, and hypoxia–ischemia in the developing brain, Free Radic. Biol. Med. 40 (2006) 388–397.
[3] C. Bonansco, M. Fuenzalida, M. Roncagliolo, Altered synaptic and electrical properties of lumbar motoneurons in the neurological glial mutant taiep rat, Exp. Brain Res. 156 (2004) 104–110.
[4] K.M. Brown, J.R. Wrathall, R.P. Yasuda, B.B. Wolfe, Quantitative measurement of glutamate receptor subunit protein expression in the postnatal rat spinal cord, Brain Res. Dev. Brain Res. 137 (2002) 127–133.
[5] D. Chao, Y. Xia, Ionic storm in hypoxic/ischemic stress: can opioid receptors subside it? Prog. Neurobiol. 90 (2010) 439–470.
[6] M. Chen, Y.X. Tao, J.G. Gu, Inward currents induced by ischemia in rat spinal cord dorsal horn neurons, Mol. Pain 3 (2007) 10.
[7] D.W. Choi, Calcium-mediated neurotoxicity: relationship to specific channel types and role in ischemic damage, Trends Neurosci. 11 (1988) 465–469.
[8] J.T. Coyle, P. Puttfarcken, Oxidative stress, glutamate, and neurodegenerative disorders, Science 262 (1993) 689–695.
[9] U. Dirnagl, C. Iadecola, M.A. Moskowitz, Pathobiology of ischaemic stroke: an integrated view, Trends Neurosci. 22 (1999) 391–397.
[10] A. Doble, The role of excitotoxicity in neurodegenerative disease: implications for therapy, Pharmacol. Ther. 81 (1999) 163–221.
[11] M.R. Hara, S.H. Snyder, Cell signaling and neuronal death, Annu. Rev. Pharmacol. Toxicol. 47 (2007) 117–141.
[12] M. Hsu, G. Buzsaki, Vulnerability of mossy fiber targets in the rat hippocampus to forebrain ischemia, J. Neurosci. 13 (1993) 3964–3979.
[13] D. Leifer, N.W. Kowall, Immunohistochemical patterns of selective cellular vulnerability in human cerebral ischemia, J. Neurol. Sci. 119 (1993) 217–228.
[14] P. Lipton, Ischemic cell death in brain neurons, Physiol. Rev. 79 (1999) 1431–1568.
[15] S.A. Lipton, P.A. Rosenberg, Excitatory amino acids as a final common pathway for neurologic disorders, N. Engl. J. Med. 330 (1994) 613–622.
[16] J.D. Marks, V.P. Bindokas, X.M. Zhang, Maturation of vulnerability to excitotoxicity: intracellular mechanisms in cultured postnatal hippocampal neurons, Brain Res. Dev. Brain Res. 124 (2000) 101–116.
[17] K. Nohda, T. Nakatsuka, D. Takeda, N. Miyazaki, H. Nishi, H. Sonobe, M. Yoshida, Selective vulnerability to ischemia in the rat spinal cord: a comparison between ventral and dorsal horn neurons, Spine 32 (2007) 1060–1066.
[18] A. Ouanonou, Y. Zhang, L. Zhang, Changes in the calcium dependence of glutamate transmission in the hippocampal CA1 region after brief hypoxia-hypoglycemia, J. Neurophysiol. 82 (1999) 1147–1155.
[19] J.E. Penny, J.R. Kukums, J.H. Tyrer, M.J. Eadie, Quantitative oxidative enzyme histochemistry of the spinal cord. Part 2. Relation of cell size and enzyme activity to vulnerability to ischaemia, J. Neurol. Sci. 26 (1975) 187–192.
[20] S.M. Rothman, Synaptic activity mediates death of hypoxic neurons, Science 220 (1983) 536–537.
[21] B. Sakmann, E. Neher, Patch clamp techniques for studying ionic channels in excitable membranes, Annu. Rev. Physiol. 46 (1984) 455–472.
[22] P.J. Shaw, C.J. Eggett, Molecular factors underlying selective vulnerability of motor neurons to neurodegeneration in amyotrophic lateral sclerosis, J. Neurol. 247 (Suppl. 1) (2000) I17–I27.
[23] E. Tanaka, S. Yamamoto, Y. Kudo, S. Mihara, H. Higashi, Mechanisms underlying the rapid depolarization produced by deprivation of oxygen and glucose in rat hippocampal CA1 neurons in vitro, J. Neurophysiol. 78 (1997) 891–902.
[24] R.J. Thompson, N. Zhou, B.A. MacVicar, Ischemia opens neuronal gap junction hemichannels, Science 312 (2006) 924–927.
[25] S. Yamamoto, E. Tanaka, H. Higashi, Mediation by intracellular calcium-dependent signals of hypoxic hyperpolarization in rat hippocampal CA1 neurons in vitro, J. Neurophysiol. 77 (1997) 386–392.

B. 神経障害性疼痛

6. 中枢性疼痛に対するケタミン点滴療法

山本隆充[1,2] 大渕敏樹[2]
小林一太[2] 大島秀規[2]
深谷 親[1,2] 片山容一[1,2]

[1]日本大学医学部先端医学系応用システム神経科学分野
[2]日本大学医学部脳神経外科学系神経外科学分野

要 旨

ケタミン点滴療法は神経障害性疼痛の治療に有用であり，central sensitization の解除にも有効と考えられる．ドラッグチャレンジテストで ketamine-sensitive な症例を対象とし，生理食塩水 100 ml にケタミン 20 mg（0.33 mg/kg）を加え，約 1 時間かけて点滴を行う．低用量ケタミン点滴療法は，2～4 週に 1 回程度の頻度で行う．長期投与でもケタミン耐性は認められず，血液・生化学検査でも異常を認めない．神経終末から興奮性アミノ酸の遊離を抑制する作用のあるガバペンチンまたはプレガバリンは，ケタミンとの併用により効果を増強することができる．さらに，脊髄刺激療法による除痛効果を高めることもできるので，低用量ケタミン点滴療法は中枢性疼痛の有力な治療方法と考える．

（ペインクリニック 31：S297-S305，2010）

キーワード：ケタミン，中枢性疼痛，ドラッグチャレンジテスト

はじめに

中枢性疼痛の中でも，求心路遮断痛は神経の損傷後に出現する疼痛を意味する．中枢性の求心路遮断痛には，視床痛，Wallenberg 症候群，脊髄損傷後疼痛などが代表例として挙げられる．また，脳卒中後疼痛は，損傷部位や出血・梗塞などの原因によって区別することなく，post-stroke pain として統一されている．

知覚求心路の切断後に中枢側ニューロンに過剰放電が出現することは，脊髄後根切断後に脊髄後角内でニューロンの過剰活動を記録した Loeser ら[1]（1967 年）の報告以来，脊髄後角，三叉神経核，視床，大脳皮質知覚野など多くの部位で確認されている[2,3]．中枢神経損傷後疼痛の出現には，i）このニューロンの過剰活動が重要な役割を担っていること，ii）このニューロンの過剰活動の発現に興奮性アミノ酸が関与していること，iii）特に知覚求心路の遮断後に著明であること，などが報告されている[4]．また，求心路遮断後に出現するニューロンの過剰活動に対して，興奮性アミノ酸の NMDA 受容体のブロッカーであるケタミンならびに興奮性アミノ酸のシナプス伝達を抑制するバルビタール薬の効果が確認されている[5-7]．臨床的にも求心路遮断後に出現する central sensitization に対するケタミンの効果が報告さ

Ketamine drip infusion therapy for post-stroke pain
Takamitsu Yamamoto, et al
Division of Applied System Neuroscience, Department of Advanced Medical Science[1], and Department of Neurological Surgery[2], Nihon University School of Medicine

れている[8,9,10]．

筆者らは，中枢性疼痛の薬理学的背景を明らかにする目的で，ドラッグチャレンジテストを行ってきた[11,12]．このドラッグチャレンジテストによってketamine-sensitiveと判定された中枢性疼痛症例についてケタミンの点滴療法を行ったので，その方法と効果について紹介する．

1．ドラッグチャレンジテスト

1）ドラッグチャレンジテストの目的と方法

中枢性疼痛の治療方針を決定するためには，ドラッグチャレンジテスト[11,12]が有用である．筆者らは，visual analogue scale（VAS）で痛みの評価を行い，薬物投与によるVASの変化を比較している．この評価法の特徴は，プラセボ投与から始め，少量ずつ段階的に薬物を投与するので，少量から連続的に多量投与までの効果を確認できることである．患者の訴える疼痛がどのような薬物にどの程度の投与量でどの程度反応するか，または全く反応しないかを明らかにすることができる．

ケタラールテストは，5分間隔で生理食塩水を2回投与後，同様に5分間隔でketamine hydrochlorideを5mg，合計25mgまで静脈内投与する．モルヒネテストは，同様に5分間隔でmorphine hydrochloride 3mgを合計18mgまで静脈内投与し，サイアミラールテストは，同様に50mgのthiamylal sodium（現在はthiopental sodium）を，5分間隔で合計250mgまで静脈内投与している．途中で入眠した場合は，その時点で中止する．（薬物投与後VAS÷薬物投与前のVAS）×100%＝%VASとして，%VASが60%以下となったもの，すなわち薬物投与前と比較して，VASが40%以上減少したものをsensitive case，40%以下のものをresistant caseとしている（図1）．

Post-stroke pain症例では，サイアミラールテストで入眠するまでVASが変化しない症例が約17%存在し，このような症例は脳脊髄刺激療法にも抵抗性であるので，脳脊髄刺激療法の患者選択のためにも有用である．

2）ドラッグチャレンジテストの対象と結果

対象は中枢性疼痛（post-stroke pain）120症例で，男性67症例，女性53症例．年齢は25歳～79歳，平均59.2歳．原因疾患は，脳梗塞37症例，脳出血83症例であった．

ケタミンテストの結果では，55症例がketamine-sensitiveで，65症例がketamine-resistantと判定された．図2はketamine-sensitive症例における経時的なVASの変化の平均値を%VASで表したものであるが，ketamine-sensitive群では，ケタラール20mgの投与によってVASが70%以上減少し，それ以上の投与量を用いても明らかな変化を認めなかった．一方，ketamine-resistant群では辺縁系に対する作用のためと考えられるが，逆にVASが増加する症例が存在した．しかし，自発痛が増加したと訴えた症例の中でも身体各部位の評価を行うと，8症例ではアロデニアが著しく抑制されていた．これらの結果を総合すると，ケタラールは120症例中63症例（52.5%）のpost-stroke painに有効であることが確認された．

3）ケタミンの副作用

5mgのケタラール[5]を5分間隔で5回静注（20分で25mg静脈内投与）するケタミンテストによって，不快な異常感覚や情動反応が出現した症例が120症例中17症例存在したが，全症例で問題なくテストを行うことができた．この17症例はいずれもketamine-resistantな症例で，ketamine-sensitiveな症例ではこのような反応を呈した症例は存在しなかった[13]．Ketamine-sensitive群では，めまい感や嘔気を訴えた症例を認めたが，ketamine-resistant群に比較すると小数であった（表1）．このような結果から，ケタミンの使用はketamine-sensitive

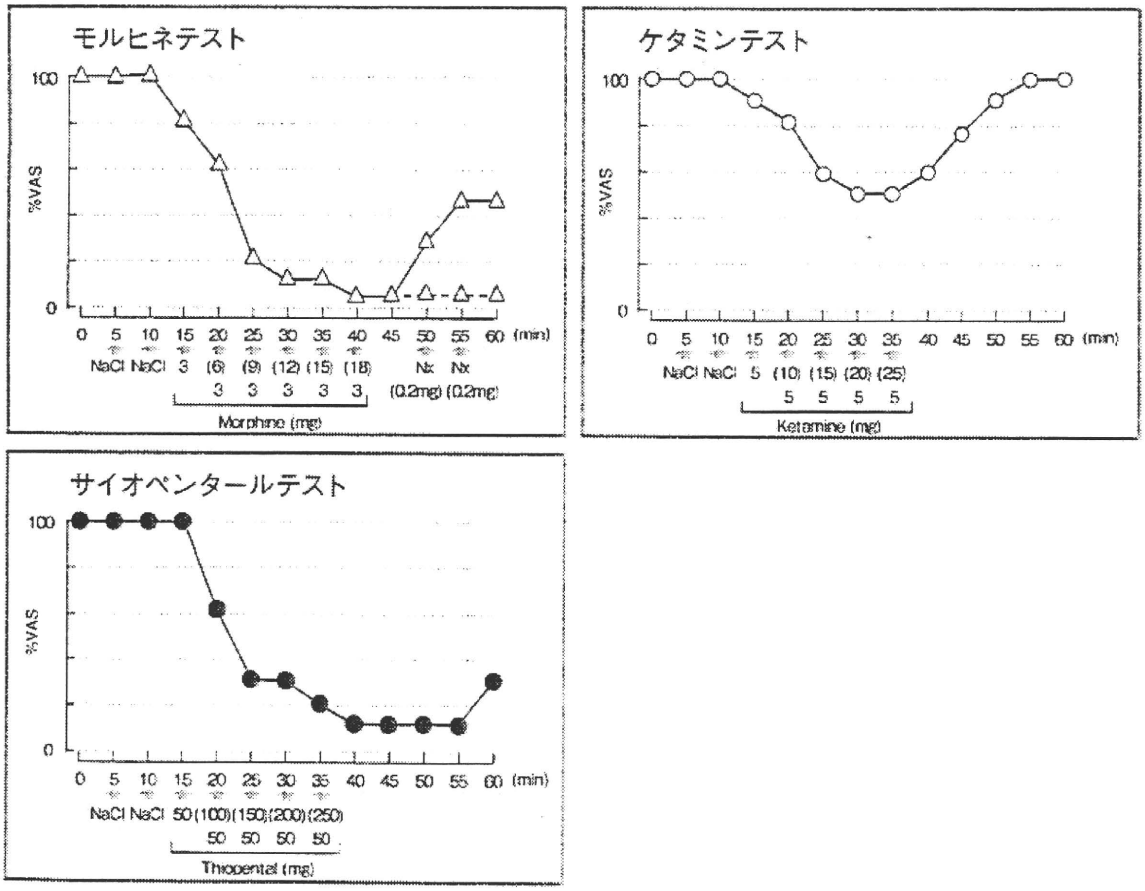

図1　ドラッグチャレンジテスト

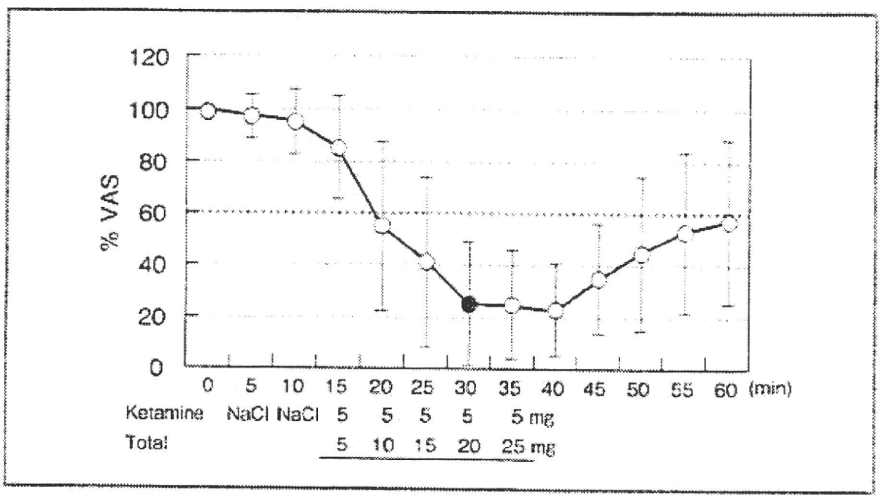

図2　ケタミンテスト

Ketamine-sensitive 症例における VAS の変化の平均値を% VAS で表したもの．この結果から低用量ケタミン点滴療法の投与量を決定した

表1　Ketamine-sensitive 群と ketamine-resistant 群でのケタミンテストによる副作用の比較

	Sensitive 群	Resistant 群
症例数	55	65
副作用の種類		
Unpleasant sensation and/or psychological reactions	0 (0 %)	17 (26.1 %)
Dizziness	2	5
Light headache	0	3
Fatigue	0	3
Nausea	1 (5.4 %)	2 (20.0 %)

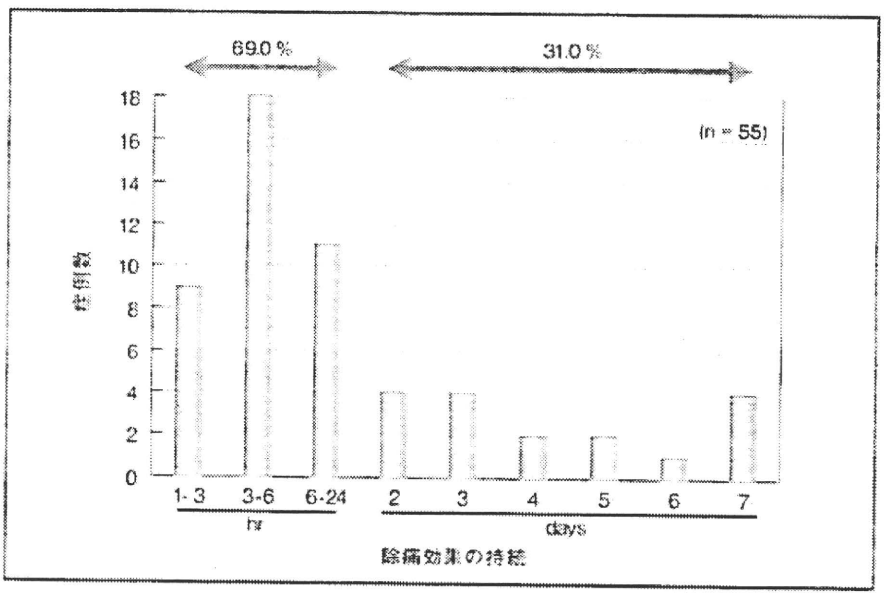

図3　低用量ケタミン点滴の除痛効果持続時間

な症例に使用すれば安全で大変に有効な方法であると考えられる[17].

4）低用量ケタミン点滴の効果

ドラッグチャレンジテストで，自発痛に対して ketamine-sensitive な post-stroke pain 55 症例に対して，低用量ケタミン点滴の効果について検討した．100 ml の生理食塩水に 20 mg (0.33 mg/kg) のケタラール® を加え，約 1 時間かけて点滴した．

この結果，除痛効果の持続は 69 % の症例が 24 時間以内であったが，31 % の症例は 24 時間以上効果が持続した（図3）．また，55 症例中 52 症例（94.5 %）が低用量ケタミン点滴の継続を希望した．除痛効果が一時的であっても，慢性的な疼痛の悪循環から解除することが重要と考えている．

表2　低用量ケタミン点滴療法

1. 生理食塩水 100 ml + ケタラール®20 mg（0.33 mg/kg） 1時間で点滴．2〜4週に1度
2. ルジオミール（Maprotiline p.o. 10〜30 mg/day）
3. レキソタン（Bromazepam p.o. 2〜6 mg/day）
4. ガバペン（Gabapentin p.o. 600〜2,400 mg/day）

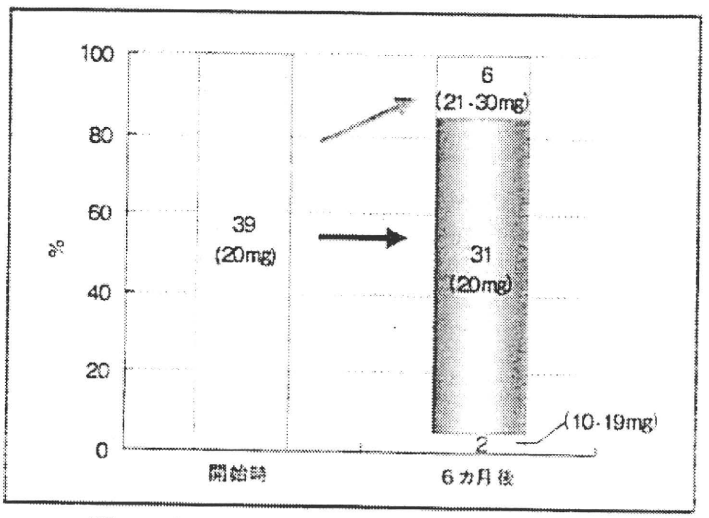

図4　長期の低用量ケタミン点滴療法による
ケタミン投与量の変化

5）低用量ケタミン点滴療法

100 ml の生理食塩水に 20 mg（0.33 mg/kg）のケタラール® を加え，約1時間かけて点滴する方法で，2〜4週間ごとに患者の希望によって行う．併用薬は塩酸マプロチニン（Ludiomil®）10〜30 mg/day，ブロマゼパム（Lexotan®）2〜6 mg/day に加えてガバペンチン（GABAPEN®）600〜2,400 mg/day を投与した．また今後は，pregabalin の併用を行う予定である．さらに，morphine-sensitive で経口オピオイドを希望した症例には経口モルヒネを投与している（表2）．

6）低用量ケタミン点滴療法の効果

Ketamine-sensitive な post-stroke pain 49 症例に対する長期的な効果について検討した．ケタミン点滴開始6カ月後に行った患者満足度調査では，疼痛のコントロールに有用であることを自覚し，6カ月以上の継続を希望したもの 39 症例（80%），疼痛のコントロールが一過性のため中止を希望したもの 10 症例（20%）であった．

長期投与によるケタミン耐性の有無についての検討では，20 mg で開始した 39 症例中，6カ月後も 20 mg が 31 症例，21〜30 mg が 6 症例，10〜19 mg が 2 症例で，モルヒネのような耐性は認めなかった（図4）．また，血液・生化学検査で異常が出現し，治療を中止した症例はいなかった．

2．ケタミン点滴療法の意義

ケタミン点滴療法では，効果の持続時間に個人差があり，わずか数時間のものから数日間持

続するものまで存在した．効果の持続時間が短い症例でも一度疼痛を軽減することが疼痛の管理には重要であり，これによって精神的な安定を得られるという症例が多い．また，central sensitization の解除にも有効であると考えられる[8-10]．ケタラールの持つ解離性麻酔薬としての性質から情動面の変化を呈する症例も存在したが，適切な投与量と投与時間を選択することによって，有効な治療効果を得ることができる．

ケタミン点滴療法の併用薬として，抗うつ薬，抗不安薬，抗てんかん薬を用いたが，三環系抗うつ薬は，脳のシナプス間隙に放出された神経伝達物質のモノアミン（NA，5-HT など）のシナプス前神経終末への再取り込みを抑制し，シナプス間隙のモノアミンを増加させることによって，シナプス後受容体に対する作用を増強するとともに，長期投与によるシナプス後受容体の減少作用（down regulation）も効果発現に関与しているものと考えられている．四環系抗うつ薬はシナプス前膜受容体，α_2受容体（自己受容体：オートレセプターとして自らNAの遊離を調整している）との結合を遮断してNAの遊離を促進することが報告されている．疼痛に対する脳幹から脊髄後核への下行性の痛み抑制に5-HTやNAが重要な役割を担っていることが実験的に証明されているが[11]，中枢性疼痛に対する下行性の痛み抑制系の関与については，現在も明確ではない．また，視床痛の症例などでは，情動失禁や痛みに対する過剰反応を呈する症例が多くみられることから，中枢神経内での痛みの認知プロセスに対する効果についても検討する必要があるものと考える．抗不安薬あるいはマイナートランキライザーと呼ばれているベンゾジアゼピン系薬物はGABA$_A$受容体のGABA親和性を高めることが報告されており，GABAの作用を増強することによって効果を発現するものと考えられている．また，バルビツール酸系薬物も同様の効果が報告されている．カルバマゼピンは抗てんかん薬であるが，三叉神経痛や求心路遮断痛に効果を認める．また，痙攣の予防にも効果を認めるとの観点から，大脳皮質運動領刺激療法を施行中の症例には特に有用性が高い．本邦でも使用可能となったガバペンチンには，神経終末からの興奮性アミノ酸の遊離を抑制する作用が報告されており，ケタミンとの相乗効果も期待される．

3．低用量ケタミン点滴療法の特徴

これまでにケタミンが麻酔薬として使用される場合は，ケタミン1～2 mg/kgを1分以上かけて静注，あるいは5～10 mg/kgを筋注する方法が用法，用量として推奨されている．一方，低用量ケタミン点滴療法は，ケタミン0.33 mg/kgを100 mlの生理食塩水に加え，1時間かけて点滴投与する方法で，全く別の使用法である．ケタミンの点滴中でも覚醒状態で患者さんの状態を確認し，精神状態ならびに疼痛の変化を確認することができる．また，求心路遮断痛では，この程度の投与量で十分な除痛効果を得ることができる．ケタミン点滴療法の明らかな除痛効果は数時間のことが多いが，疼痛が持続して難治性となっている症例においては，一時的であっても疼痛から開放される時間を提供することによって，増大した痛みの感覚をリセットすることができ，日常の生活も改善される[15-18]．さらに，抗うつ薬，抗不安薬，抗痙攣薬の内服を併用することによって，持続的な除痛効果を得ることができ，患者さんの負担も少なく，日常の生活改善を図ることができる．

4．Dual-lead SCS と low-dose ketamine 点滴療法の併用効果

Dual-lead spinal cord stimulation（図5）の効果を，VASの減少率を基に，Excellent（60%以上），Good（30～59%），Fair（29%未満）に分類すると，post-stroke pain では Excel-

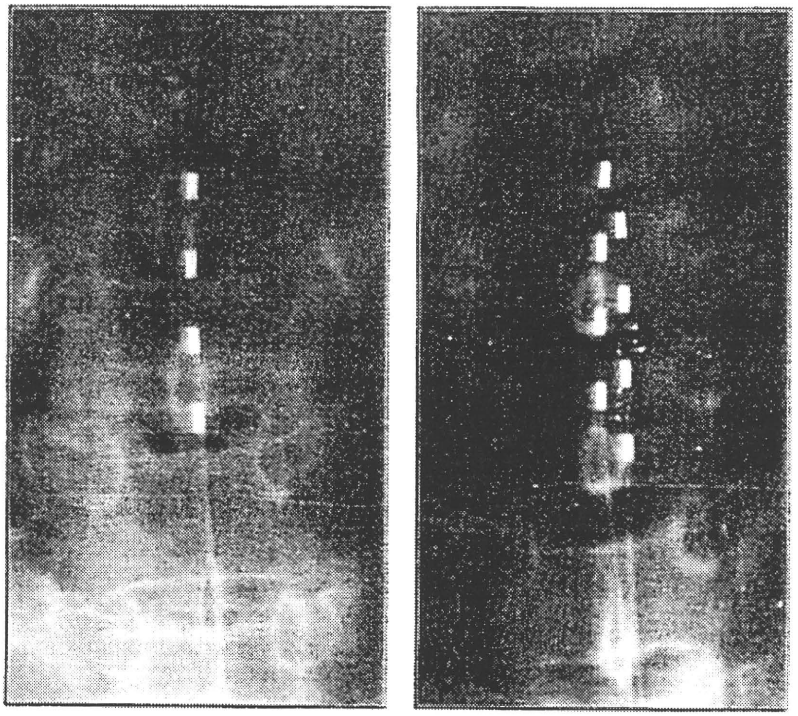

Single-lead SCS　　Dual-lead SCS

図5　Single-lead SCS と Dual-lead SCS

Dual-lead SCS は2本の刺激電極を1つの刺激装置と結線して使用するので，電極間の刺激を行うこともできる．これによって，疼痛部に刺激の paresthesia を誘発するのが容易になった

表3　各種の神経障害性疼痛に対する Dual-lead SCS の効果

Post-stroke pain 症例に対しても，Dual-lead SCS と低用量ケタミン点滴療法の併用によって，疼痛を軽減することができる症例が多く存在する

原　因	植込み数/試験刺激数	Excellent	Good	Fair
Post-stroke pain	12/16	2	6	4
Failed-back pain	4/5	1	2	1
CRPS	3/3	2	1	
Post-myelitis	1/1		1	
Phantom limb pain	1/1		1	
Nerve injury	2/2	1	1	
Parkinson Disease	1/1		1	
	24/29 (83%)	6	13	5
		19/24 (79%)		5/24 (21%)

Excellent：over 60% VAS reduction
Good：30-59% VAS reduction
Fair：under 29% VAS reduction

lent 2症例，Goodが6症例，Fair 4症例．Failed-back painではExcellent 1症例，Good 2症例，Fair 1症例，CRPSではExcellent 2症例，Good 1症例，Post-myelitisではGood 1症例，phantom limb painではGood 1症例，Peripheral Nerve injuryではExcellent 1症例，Good 1症例，Parkinson病の疼痛ではGood 1症例であった（表3）．34症例の中で，VASの減少率からdual-lead SCSの効果がFairと判定されたものが5症例存在したが，これらの症例も含めて全症例でlow-dose ketamine点滴後には著しい疼痛の軽減を認め，dual-lead SCSの効果増強も自覚することができた[19]．テスト刺激から慢性植え込みに移行する症例が83%と高率であった理由としては，ドラッグチャレンジテストによる患者選択の有用性が考えられる．

まとめ

低用量ケタミン点滴療法は，post-stroke painなどの中枢性疼痛ならびに末梢性の神経障害性疼痛の軽減に有効であり，脳脊髄刺激療法の効果を高めることもできる．ドラッグチャレンジ・テストは治療方針の決定に大変有用であり，この結果に基づいて低用量ケタミン点滴療法を行うことにより，難治性と考えられる中枢性疼痛の治療成績を向上させることができる．

文献

1) Loeser JD, Ward AA: Some effects of deafferentation on neurons of the cat spinal cord. Arch Neurol 17: 48-50, 1967
2) Koyama S, Katayama Y, Maejima S, et al: Thalamic neuronal hyperactivity following transaction of the spinothalamic tract in the cat: Involvement of *N*-methyl-D-aspartate receptor. Brain Res 612: 345-350, 1993
3) Lenz FA, Kwan HC, Martin R, et al: Characteristics of somatotopic organization and spontaneous neuronal activity in the region of the thalamic principal sensory nucleus in patients with spinal cord transaction. J Neurophysiol 72: 1570-1587, 1994
4) Coderre T, Katz J, Vaccarino AL, et al: Contribution of central neuroplasticity to pathological pain: Review of clinical and experimental evidence. Pain 52: 259-285, 1993
5) Cai Z, McCaslin PP: Acute, chronic and differential effects of several anaesthetic barbiturates on glutamate receptor activation in neural culture. Brain Res 611: 181-186, 1993
6) Gerber G, Randic M: Participation of excitatory amino acid receptors in the slow excitatory synaptic transmission in the rat spinal cord *in vitro*. Neurosci Lett 70: 143-147, 1986
7) Oye I, Paulsen O, Maurset A: Effects of ketamine on sensory perception: Evidence for a role of *N*-methyl-D-aspartate receptors. J Pharmacol Exp Ther 260: 1209-1213, 1992
8) Person J, Axelsson G, Hallin RG, et al: Beneficial effects of ketamine in a chronic pain state with allodynia, possibly due to central sensitization. Pain 60: 217-222, 1995
9) Jorum E, Warncke T, Stubhang A: Cold allodynia and hyperalgesia in neuropathic pain: The effect of *N*-methyl-D-aspartate (NMDA) receptor antagonist ketamine: A double-blind, cross-over comparison with alfentanil and placebo. Pain 101: 229-235, 2003
10) Kvarnstrom A, Karlsten R, Quiding H, et al: The analgesic effect of intravenous ketamine and lidocaine on pain after spinal cord injury. Acta Anaesthesiol Scand 48: 498-506, 2004
11) Yamamoto T, Katayama Y, Tsubokawa T, et al: Usefulness of the morphine/ thiamylal test for the treatment of deafferentation pain. Pain Res 6: 143-146, 1991
12) Yamamoto T, Katayama Y, Hirayama T, et al: Pharmacological classification of central post-stroke pain: Comparison with the results of chronic motor cortex stimulation therapy. Pain 72: 5-12, 1997
13) Yamamoto T, Katayama Y, Obuchi T, et al: Drug-challenge test and drip infusion of ketamine for post-stroke pain. Pain Research 24: 191-199, 2009
14) Fields HL, Anderson SD: Evidence that raphe-spinal neurons mediate opiate and midbrain stimulation-produced analgesia. Pain 5: 333-349, 1978
15) Nikolajsen L, Hansen CL, Nielsen J, et al: The effect of ketamine on phantom pain: A cen-

tral neuropathic disorder maintained by peripheral input. Pain 67:69-77, 1996
16) Backonja M, Arndt G, Gombar KA, et al:Response of chronic neuropathic pain syndromes to ketamine:A preliminary study. Pain 56:51-57, 1994
17) Mathisen LC, Skjelbred P, Skoglund LA, et al:Effect of ketamine, an NMDA receptor inhibitor, in acute and chronic orofacial pain. Pain 61:215-220, 1995
18) Felsby S, Nielsen J, Arendt-Nielsen L, et al: NMDA receptor blockade in chronic neuropathic pain:A comparison of ketamine and magnesium chloride. Pain 64:283-291, 1995
19) 山本隆充，大渕敏樹，加納利和，他：神経障害性疼痛に対するDual-leadを用いた脊髄刺激療法とlow-dose ketamine点滴療法の併用効果．Pain Research 24:9-15, 2009

※　　※　　※

Int J Biometeorol (2011) 55:319–326
DOI 10.1007/s00484-010-0339-8

ORIGINAL PAPER

The rate and magnitude of atmospheric pressure change that aggravate pain-related behavior of nerve injured rats

Megumi Funakubo · Jun Sato · Kouei Obata · Kazue Mizumura

Received: 8 March 2010 / Revised: 27 May 2010 / Accepted: 2 June 2010 / Published online: 24 June 2010

Abstract Complaints of patients with chronic pain may increase when the weather changes. The exact mechanism for weather change-induced pain has not been clarified. We have previously demonstrated that artificially lowering barometric pressure (LP) intensifies pain-related behaviors in rats with neuropathic pain [chronic constriction injury (CCI) and spinal nerve ligation (SNL)]. In the present study, we examined the rate and magnitude of LP that aggravates neuropathic pain. We measured pain-related behaviors [number of paw lifts to von Frey hair (VFH) stimulation] in awake rats after SNL or CCI surgery, and found that rates of decompression ≥5 hPa/h and ≥10 hPa/h and magnitudes of decompression ≥5 hPa and ≥10 hPa augmented pain-related behaviors in SNL and CCI rats, respectively. These results indicate that LP within the range of natural weather patterns augments neuropathic pain in rats, and that SNL rats are more sensitive to LP than CCI rats.

Keywords Weather-sensitive pain · Decompression rate · Decompression magnitude · Low pressure exposure · Rats

M. Funakubo · K. Mizumura (✉)
Department of Neuroscience II,
Research Institute of Environmental Medicine,
Nagoya University,
Furo-cho, Chikusa-ku,
Nagoya 464-8601, Japan
e-mail: mizu@riem.nagoya-u.ac.jp

J. Sato
Futuristic Environmental Simulation Center,
Research Institute of Environmental Medicine,
Nagoya University,
Furo-cho, Chikusa-ku,
Nagoya 464-8601, Japan

K. Obata
R & D Department, Environmental Technology Laboratory,
Daikin Industries, Ltd.,
1304 Kanaoka-cho, Kita-ku, Sakai-shi,
Osaka 591-8511, Japan

Present Address:
M. Funakubo
Department of Neurology, School of Medicine, Keio University,
35 Shinanomachi, Shinjuku-ku,
Tokyo 160-8582, Japan

Introduction

Some meteorological factors, e.g., barometric pressure, humidity, and temperature, influence chronic pain (Mitchell 1877; Hollander and Yeostros 1963; Kranzl 1977; Guedj and Weinberger 1990; Hendler et al. 1995, Jamison et al. 1995; Verges et al. 2004). This symptom is called "weather-sensitive pain". Many patients with chronic pain from such conditions as rheumatoid arthritis, low back pain, and neuropathic pain complain that their condition is aggravated by changes in the weather (Mitchell 1877; Hollander and Yeostros 1963; Kranzl 1977; Guedj and Weinberger 1990; Hendler et al. 1995; Jamison et al. 1995; Verges et al. 2004).

We have previously examined the effects of lowering barometric pressure (LP) and lowering ambient temperature (LT; by 7°C from 22°C) on pain-related behaviors in animals in which psychosocial factors are considered minimal (Sato 2003; Sato et al. 2004), and have demonstrated that LP (27 hPa decrease in 8 min) or LT augment pain-related behaviors of chronic constriction injury (CCI) rats (Sato et al. 1999, 2000) and adjuvant-inflamed rats but had no effect on sham operated rats (Sato et al. 2004). We also showed that the inner ear played a pivotal role in this

effect (Funakubo et al. 2010). Although the magnitude of LP used was within the range of naturally occurring changes, the rate of LP was much faster than that of natural change. Since the changing rate of barometric pressure might strongly influence the LP effect on pain, we examined in this experiment the effects of a range of LP at different rates and magnitudes using a newly constructed decompression chamber that decreases the atmospheric pressure much more slowly (0.2–150 hPa/h) than the previous one (Funakubo et al. 2010).

Our previous study has also demonstrated the involvement of sympathetic nerve activities in LP-induced pain aggravation (Sato et al. 1999). In addition, there are reports showing different contributions of sympathetic nerve activities in different models of neuropathic pain, e.g., a higher contribution in the spinal nerve ligation (SNL) model than in the CCI model (Kim et al. 1997). From these results, it would be reasonable to expect that different pain models with different involvement of sympathetic nerve activities might show some difference in LP sensitivity. Therefore, in this experiment, we examined the effects of LP in both SNL and CCI models.

Materials and methods

Thirty-four male Sprague-Dawley (SD) rats, 250–300 g (Japan SLC) were used. The animals were housed two to three per cage under a controlled temperature (24°C) and on a 12-h light/dark cycle (7:00~19:00/19:00~7:00), and were given free access to food and water. All surgical procedures described below were performed under surgically clean conditions and sodium pentobarbital anesthesia (50 mg/kg, i.p.). All the experiments were conducted according to the Regulations for Animal Experiments in Nagoya University, and the Fundamental Guidelines for Proper Conduct of Animal Experiments and Related Activities in Academic Research Institutions in Japan.

SNL surgery

The left L5 spinal nerve was tightly ligated with silk thread according to the method described by Kim and Chung (1992), except that only the L5 spinal nerve was ligated in the present experiment.

CCI surgery

CCI surgery was performed according to the method previously described (Bennett and Xie 1988). Briefly, the left sciatic nerve was exposed at the mid-thigh level, and was then constricted with four loose ligatures using chromic gut (4/0), each spaced about 1 mm apart.

Measurement of pain-related behaviors

Behavior tests were carried out between 9:00 and 18:00 during the light phase.

Measurement of punctate hyperalgesia

Mechanical hyperalgesia developed 3 days after CCI or SNL surgery. We confirmed that rats remained hyperalgesic at least for 3 weeks thereafter (Jin et al. 2008, and unpublished observation from our laboratory) while rats with sham surgery were not hyperalgesic. Therefore, experiments were done between 6 and 22 days after CCI surgery or 5 and 21 days after SNL surgery.

Each rat was individually placed beneath an inverted transparent plastic cage (11×17×11 cm) with a wire mesh bottom. Pain-related behaviors induced by mechanical stimulation were measured with home-made von Frey hairs (VFHs; diameter: 0.5 mm, bending forces 34.3, 92.2, 197.2 mN). Each VFH was applied ten times (once every 2–3 s) to the plantar surface of the nerve-injured paw, and

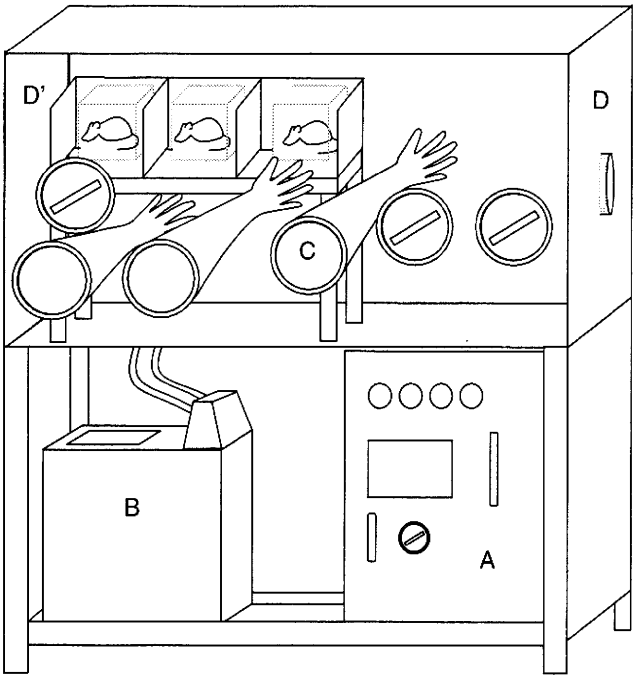

Fig. 1 Schema of the small pressure-controlled chamber used. Barometric pressure in this chamber can be reduced at a variety of rates (0.2–150 hPa/h), and can be maintained at a given value (960–1030 hPa) by a vacuum pump (*A*). The chamber size is 1500×750×550 mm (W/H/D). Its three sides are made of transparent acrylic resin, and the experimenter can handle animals in the chamber and perform pain tests through gloves (*C*) while directly observing the subjects. The temperature and the humidity can be maintained at a constant level (22±2°C, 50±10%) by a temperature-controlled bath (*B*). The windows on both sides (*D* and *D'*) are detachable, allowing experimental animals and testing devices to be placed in and removed from the chamber

the number of foot withdrawals was then counted (Zhou et al. 1996; Ta et al. 2000). Stimulation of normal human skin with the weak (34.3 mN) and then stronger (92.2 and 197.2 mN) VFHs elicits a sensation of pressure and painful pricking, respectively. An increased number of foot withdrawals following mechanical stimulation of the foot skin means hyperalgesia (Zhou et al. 1996; Ta et al. 2000).

Threshold measurement

VFHs were applied perpendicular to the plantar surface of the left hind paw through the wire mesh with sufficient force to cause slight bending against the paw. The hairs were applied in the order of increasing bending force (10 steps from 18.1 to 387.1 mN in quasi-logarithmic scale), with each applied five times at intervals of 2–3 s to different parts of the midplantar glabrous skin. The strength of the first hair in the series that evoked at least one positive response among the five trials was designated the pain threshold.

Low-pressure (LP) exposure

We examined the range of the rate and magnitude of barometric pressure changes that aggravate neuropathic pain. For this, we used a pressure-controlled chamber, newly constructed by Daikin Industries, Ltd. R & D Dept., as schematically shown in Fig. 1. This chamber is able to lower the barometric pressure at a variety of rates and ranges. Controllable pressure range is 960–1030 hPa, with the rate 0.2–150 hPa/h. The chamber size is 1,500×750×550 mm (W/H/D). The rats were handled and stimulated by an experimenter through air-tight rubber gloves (C in Fig. 1). On opening the cover of a glove attached to the chamber wall, pressure increase occurred, and its magnitude depended on the pressure difference between the inside and the outside of the chamber. Therefore, covers of the gloves that were expected to be used during the experiment were removed before starting pressure decrease. When an experimenter inserted her hand into the gloves, brief pressure increase <2 hPa was observed (marked with an arrow in Fig. 2a-i). This small pressure increase did not induce any visible change in rat behavior. Figure 2a-i, ii show pressure recordings during, respectively, the fastest and slowest pressure changes that were performed on different days with different natural atmospheric pressure. In spite of difference in their baselines, the pressure inside the chamber was well controlled according to the demand except when an experimenter inserts her hand into the glove (arrow, described above). The temperature and the

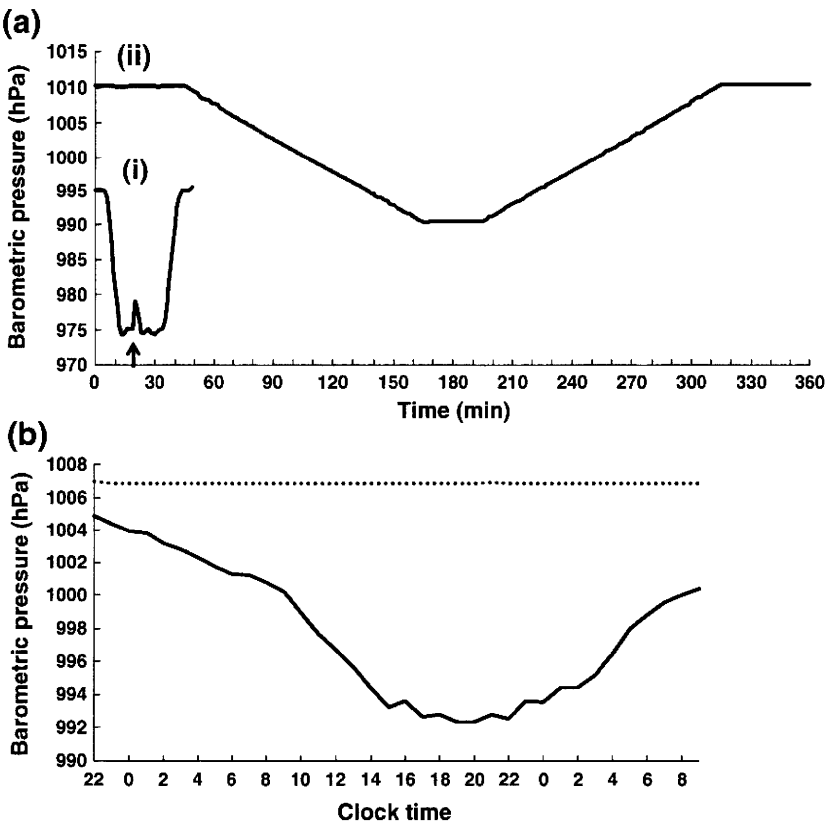

Fig. 2 Recordings of barometric pressure in the chamber. **a** Recordings of barometric pressure in the chamber when it was set to decrease by 20 hPa over 14 min (*i*), i.e. 86 hPa/h, and over 2 h (*ii*), i.e. 10 hPa/h. Moving two gloves as in the behavior test, pressure changes in the range of 2 hPa (*arrow*). **b** Change of atmospheric pressure when a typhoon passed by Nagoya (Typhoon No.18. September 7, 2004). Atmospheric pressure outside the chamber (*solid line*), controlled barometric pressure in the chamber when it was set to 1,007 hPa (*dotted line*). *Horizontal axis* shows time of day. This chamber was able to maintain the pressure level when the outside atmospheric pressure changed significantly

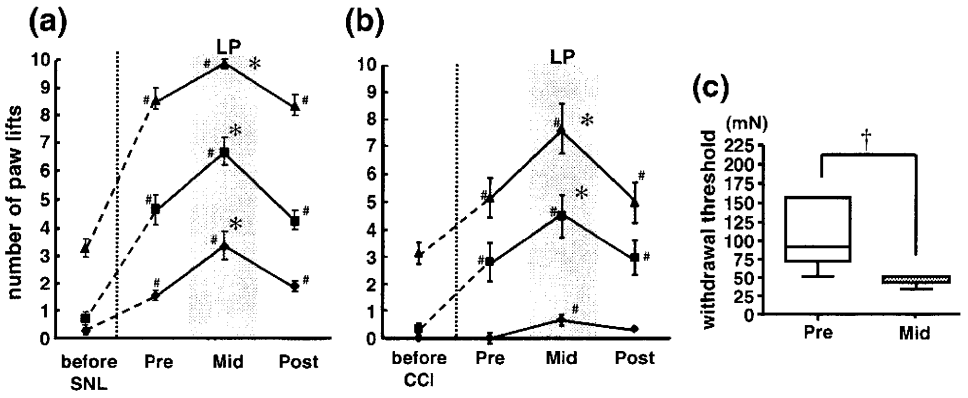

Fig. 3 Nerve injury-and low pressure exposure-induced changes in number of paw lift to VFH stimulation. **a** An increased number of paw lifts to VFH stimulation after SNL surgery was further increased immediately after reaching the LP level (n=9). *Ordinate* number of paw lifts responding to 10 applications of a certain VFH, *abscissa* time point of testing. *Gray area* period for LP exposure (same in **b**). *Solid diamond* response to the weak von Frey hair (34.3 mN), *solid square* response to 92.2 mN hair, *solid triangle* response to 197.2 mN hair. *Before SNL* mean value of 1 and 2 days before SNL operation, *Pre* 60 min before LP exposure, *Mid* within 20 min after reaching LP, *Post* 60 min after LP exposure. $^{\#}P<0.05$, compared with the value before SNL, $^{*}P<0.05$, compared with Pre value (Student-Newman-Keuls Method). **b** Increased number of paw lifts to VFH stimulation further increased after reaching the LP level in CCI rats (n=6). $^{*}P<0.05$, compared with Pre value (Student-Newman-Keuls Method). **c** Cutaneous mechanical withdrawal threshold measured with von Frey hairs in CCI rats decreased after reaching the LP level. Data are presented as *box* (median ± interquartile range (IQR) and *whiskers* (10 and 90 percentile values). *Ordinate* withdrawal threshold in mN, *abscissa* time point of testing. LP by 20 hPa at the rate of 10 hPa/h decreased the mechanical threshold. $^{\dagger}P<0.05$, compared with Pre value (n=6, Wilcoxon's signed rank test)

humidity were maintained at a constant level (22±2°C, 50±10%). Figure 2b shows actual recording of the atmospheric pressure outside the chamber (solid line) and of the controlled barometric pressure changes inside the chamber (dotted line) on the day a major typhoon was coming. During approach of the typhoon, the atmospheric pressure decreased by 13 hPa while the barometric pressure inside the chamber was maintained constant. From these results, it is evident that the chamber used in the present experiment is capable of maintaining its own barometric pressure independent of atmospheric pressure changes outside.

Before the experiments, the rats were acclimated in the chamber (ambient temperature 22±2°C, relative humidity 50±10%) for 60 min and then exposed to falling barometric pressure (LP) of various magnitudes (3–20 hPa) at different rates of pressure change (4–86 hPa/h). Except otherwise noted, behavioral tests were carried out three times; before (Pre), immediately after reaching the pre-set LP level (Mid) and after (Post) barometric pressure fall. In the previous study, we observed that rats showed an increased number of paw lifts in response to noxious stimuli immediately after the chamber pressure had reached its lowest level. However, the increased paw lifts disappeared when tested again 60 min afterwards under the same LP conditions (Sato et al. 1999). Thus, the behavior test was carried out only once immediately after reaching the lowest barometric pressure.

A group of animals was placed in the chamber without changing pressure, and nociceptive behavior was tested using the same schedule as described above; this group served as the control (CTR).

Statistical analysis

The results of LP exposure over a variety of magnitudes and rates were expressed as the mean and standard errors of the mean (SEM). Relative increases or decreases in the number of paw lifts in response to VFH stimulation (Δnumber of paw lifts) were obtained from the value before (Pre) and during (Mid) the exposure, and analyzed using a Wilcoxon's signed rank test except when otherwise noted.

Results

Punctate hyperalgesia during LP exposure

Figure 3a shows the results of nociceptive aggravation during LP exposure in the SNL rats (LP by 10 hPa at the rate of 10 hPa/h). After SNL surgery, an increased number of paw lifts was observed at all three stimulation intensities (the upper, middle and lower lines) of VFH stimulation when compared with the corresponding pre-surgery baselines. Upon exposure to LP (Mid), SNL rats showed a further increase in the number of the paw lifts in response to VFH stimulation. The increased paw lift response returned to its pre-LP baseline levels shortly after the chamber LP was restored to its pre-LP levels (Post). It could be noted that CCI rats subjected to the same LP exposure gradation showed much the same responses of aggravation of pain-related behavior (Fig. 3b). There was

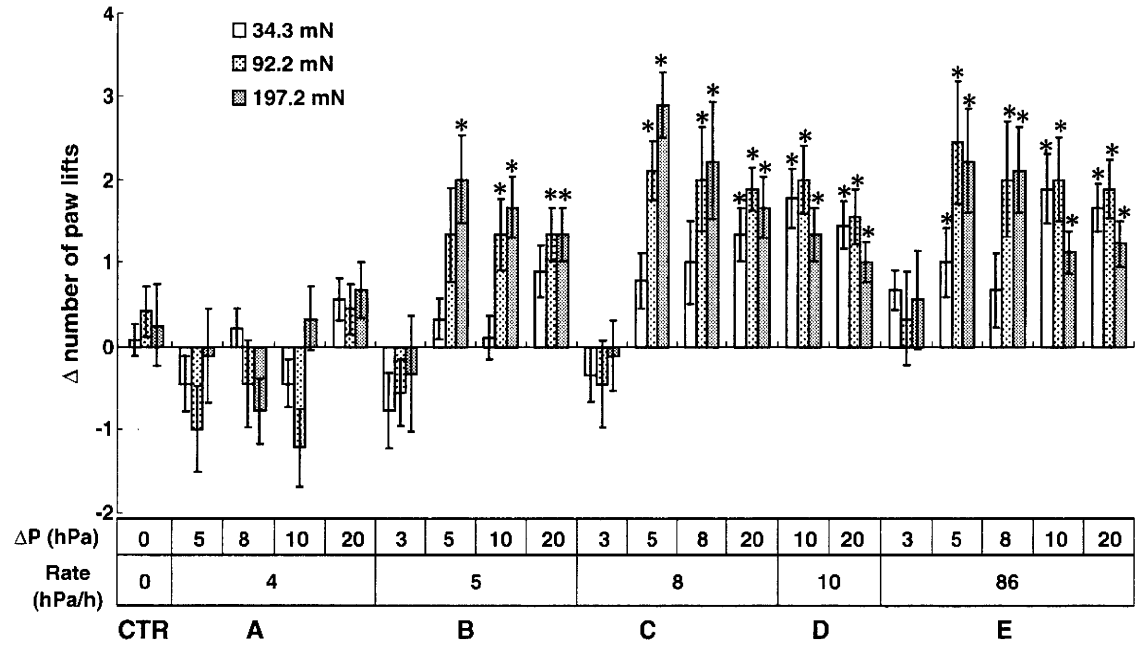

Fig. 4 Effects of various rates and magnitudes of pressure change on pain-related behavior of SNL rats. Each *column* shows the increase or decrease in the number of paw lifts to VFH stimulation during LP at various rates from 'Pre' value in the SNL rats (n=9, mean ± SEM). Control values obtained from the study in which animals were put in the chamber but without LP exposure, are also shown (*CTR*; n=12). ΔP magnitude of barometric pressure decrease. *P<0.05 compared with the 'Pre' value (Wilcoxon's signed rank test). LP by ≥5 hPa at the rate of ≥5 hPa/h increased the number of paw lifts in SNL rats

no significant change in pain-related behaviors when animals were placed in the chamber without a pressure change (data not shown).

The threshold change was studied in CCI rats only, because the threshold of SNL rats is too low to measure with our VFHs. Figure 3c shows the results of this change

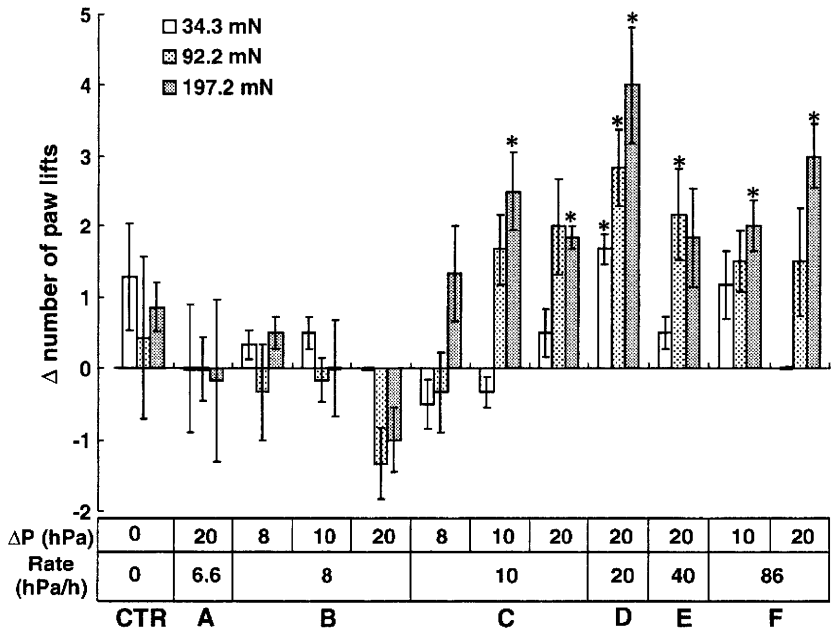

Fig. 5 Effects of various rates and magnitudes of pressure change on pain-related behavior of CCI rats. The manner of presentation is the same as in Fig. 4 (n=6) except grouping. Control values obtained from the study without LP are also shown (*CTR*; n=7). ΔP by ≥10 hPa at the rate of ≥10 hPa/h increased the number of paw lifts in CCI rats

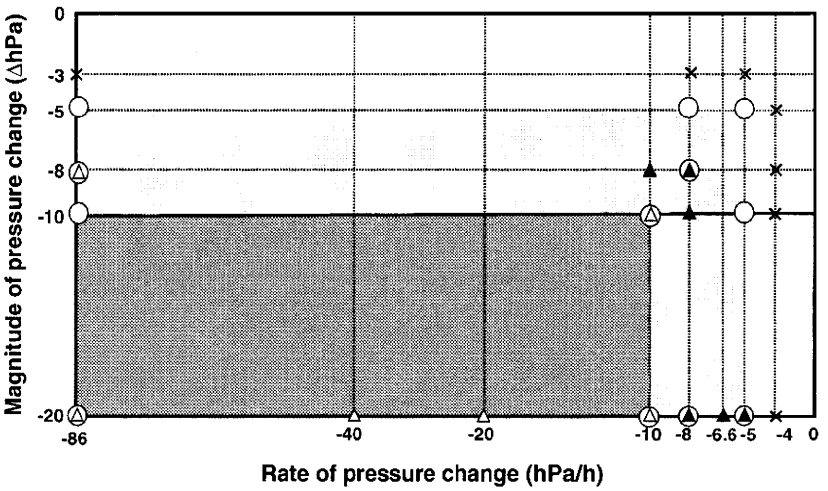

Fig. 6 Comparison between CCI and SNL rats in the rate and magnitude of effective decompression for aggravating pain-related behavior. *Abscissa* rate of pressure decrease in hPa/h, *ordinate* pressure decrease in hPa. *Open triangle* pain-related behaviors are significantly augmented in CCI rats (n=6), *filled triangle* without any significant changes in CCI rats (n=6). *Open circle* pain-related behaviors are significantly augmented in SNL rats (n=9), *cross* without any significant changes in SNL rats (n=9). LP at the rate of ≥5 hPa/h increased the number of paw lifts in SNL rats. *Dark gray area* range where aggravation of pain-related behaviors was observed in CCI rats, *gray area* range where such aggravation was observed in SNL rats

during LP exposure (by 20 hPa at the rate of 10 hPa/h) in CCI rats. LP significantly decreased the withdrawal threshold. The median values of the threshold was 92.2 mN (IQR: 92.2–140.8) and 52 mN (IQR: 52–52) before (Pre) and after the pressure reached the bottom (Mid), respectively.

Rate and magnitude of pressure decrease inducing aggravation of pain-related response

In SNL rats, we varied the magnitude of the pressure decrease between 3 hPa to 20 hPa, and the rate of changing pressure between 3 to 86 hPa/h. At a rate of 4 hPa/h, none of the pressure decreases ranging between 5 and 20 hPa induced any significant increase in the number of paw lifts (group A in Fig. 4). However at the rate 5 hPa/h or faster (groups B–E in Fig. 4), pressure reduction in these ranges induced a significant rise in the number of paw lifts responding to VFH 92.2 mN and 197.2 mN, whereas a 3 hPa decrease was ineffective at any rate of pressure decrease used. A stronger (10 and 20 hPa) and faster pressure decrease (≥8 hPa/h) induced increases in the number of paw lifts also responding to the weakest VFH stimulation. Thus, decompression rates of 5 hPa/h or faster and pressure changes of 5 hPa or larger were necessary to induce a significant increase in the number of paw lifts responding to VFH stimulation in SNL rats.

In CCI rats, sensitivity to LP was somewhat less than that in SNL rats: the level of decompression sufficient to induce pain aggravation was 10 hPa or larger, and the effective decompression speed was 10 hPa/h (Fig. 5) or faster. An increase in the number of paw lifts in CCI rats was mainly observed in response to the strongest VFH (197.2 mN), whereas SNL rats showed an increased response to the mid-strength VFH (92.2 mN), and even to the weakest one as well at the stronger and faster drops in pressure (Fig. 4). The difference in sensitivity to barometric pressure changes between SNL and CCI rats is clearly seen in Fig. 6. The dotted area denotes the magnitude (ordinate) and the rate (abscissa) of decompression that induced aggravation of pain-related behavior in CCI rats, while the gray area denotes those in SNL rats. It is clear the SNL rats are more sensitive to barometric pressure changes in both magnitude and rate of decrease than the CCI rats.

Discussion

In our previous study, we examined the lowering pressure-induced aggravation of pain-related behavior of neuropathic pain models in a climate-controlled room installed in our Institute (Sato et al. 1999, 2001, 2004). The slowest speed and smallest magnitude for this chamber to decrease atmospheric pressure was 27 hPa in 8 min. These changes (27 hPa in 202.5 hPa/h) are far greater than the naturally occurring changes. Therefore, in the present experiment, we introduced a new pressure-controlled chamber that enabled much smaller and much slower pressure changes.

The present results demonstrated that decompression rates ≥5 hPa/h and decompression magnitude ≥5 hPa caused a significant augmentation of pain-related behavior